45. A. Ferre-D'Amare, K. Zhou, J. A. Doudna, *Nature* **395**, 567 (1998).
46. S. Nakano, D. M. Chadalavada, P. C. Bevilacqua, *Science* **287**, 1493 (2000).
47. A. T. Perrotta, I.-h. Shih, M. D. Been, *Science* **286**, 123 (1999).
48. T. A. Steitz and R. G. Shulman, *Annu. Rev. Biophys. Bioeng.* **11**, 419 (1982).
49. D. E. Koshland Jr., *Cold Spring Harbor Symp. Quant. Biol.* **28**, 473 (1963).
50. W. S. Bennett Jr. and T. A. Steitz, *Proc. Natl. Acad. Sci. U.S.A.* **75**, 4848 (1978).
51. J. H. Cate, M. M. Yusupov, G. Z. Yusupova, T. N. Earnest, H. F. Noller, *Science* **285**, 2095 (1999).
52. P. B. Moore, in *Ribosomal RNA & Structure, Evolution, Processing and Function in Protein Biosynthesis*, R. A. Zimmermann and A. E. Dahlberg, Eds. (CRC Press, Boca Raton, FL, 1996), pp. 199–236.
53. P. Nissen, M. Kjeldgaard, S. Thirup, B. F. C. Clark, J. Nyborg, *Biochimie* **78**, 921 (1996).
54. D. Moazed and H. F. Noller, *Nature* **342**, 142 (1989).
55. W. D. Picking, W. L Picking, O. W. Odonu, B. Hardesty, *Biochemistry* **31**, 2368 (1992).
56. G. Blobel and D. D. Sabatini, *J. Cell. Biol.* **45**, 130 (1970).
57. C. Chothia and J. Janin, *Nature* **256**, 705 (1975).
58. Z. Xu and P. B. Sigler, *J. Struct. Biol.* **124**, 129 (1998).
59. A. Prinz, C. Behrens, T. A. Rapoport, E. Hartmann, K.-U. Kalies, *EMBO J.* **19**, 1900 (2000).
60. B. Dobberstein, personal communication.
61. B. Zhaug and T. R. Cech, *Chem. Biol.* **5**, 539 (1998).
62. M. Welch, I. Majerfeld, M. Yarus, *Biochemistry* **36**, 6614 (1997).
63. M. Carson, *Methods Enzymol.* **227**, 493 (1997).
64. We thank B. Freeborn for her skilled technical assistance in preparing 50S ribosomal subunit material and crystals. We thank M. Yarus for his generous gift of CCdA-p-puromycin, and S. Strobel, J. Steitz, D. Crothers, D. Herschlag, and T. Cech for discussions. We are indebted to R. Sweet and M. Capel for their assistance with data collection at the National Synchrotron Light Source (Brookhaven National Laboratory), and A. Joachimiak and the staff of 19-ID at the Advanced Photon Source (Argonne National Laboratory). Supported by grants from NIH to T.A.S. (GM22778) and P.B.M. (GM54216) and a grant from the Agouron Institute to T.A.S. and P.B.M. N.B. is supported by a Burroughs Welcome Fund Career Award. Coordinates of the ligand-free subunit and of domain V complexed with the two analogs have been deposited in the Protein Data Bank with accession numbers 1FFK, 1FFZ, and 1FG0.

10 July 2000; accepted 24 July 2000

REPORTS

Magnetic Vortex Core Observation in Circular Dots of Permalloy

T. Shinjo,[1]* T. Okuno,[1] R. Hassdorf,[1]† K. Shigeto,[1] T. Ono[2]

Spin structures of nanoscale magnetic dots are the subject of increasing scientific effort, as the confinement of spins imposed by the geometrical restrictions makes these structures comparable to some internal characteristic length scales of the magnet. For a vortex (a ferromagnetic dot with a curling magnetic structure), a spot of perpendicular magnetization has been theoretically predicted to exist at the center of the vortex. Experimental evidence for this magnetization spot is provided by magnetic force microscopy imaging of circular dots of permalloy ($Ni_{80}Fe_{20}$) 0.3 to 1 micrometer in diameter and 50 nanometers thick.

Ferromagnetic materials generally form domain structures to reduce their magnetostatic energy. In very small ferromagnetic systems, however, the formation of domain walls is not energetically favored. Specifically, in a dot of ferromagnetic material of micrometer or submicrometer size, a curling spin configuration—that is, a magnetization vortex (Fig. 1)—has been proposed to occur in place of domains. When the dot thickness becomes much smaller than the dot diameter, usually all spins tend to align in-plane. In the curling configuration, the spin directions change gradually in-plane so as not to lose too much exchange energy, but to cancel the total dipole energy. In the vicinity of the dot center, the angle between adjacent spins then becomes increasingly larger when the spin directions remain confined in-plane. Therefore, at the core of the vortex structure, the magnetization within a small spot will turn out-of-plane and parallel to the plane normal. Although the concept of such a magnetic vortex with a turned-up magnetization core has been introduced in many textbooks (*1*), direct experimental evidence for this phenomenon has been lacking.

Recent model calculations for a Heisenberg spin system of $32 \times 32 \times 8$ spins in size (*2*) indicate that a curling spin structure is realized even for a dot of square shape, where a spot with turned-up magnetization normal to the plane exists at the center of the vortex (Fig. 1). The simulations, which are based on a discrete-update Monte Carlo method described elsewhere (*3*), take account of exchange and dipole energies while neglecting anisotropy. Further, they show that no out-of-plane component of the magnetization occurs if the dot thickness becomes too small. On the other hand, when the thickness exceeds a certain limit, the top and bottom spin layers will tend to cancel each other, and again no perpendicular magnetization should be observed. A vortex core with perpendicular magnetization is therefore expected to appear if the shape, size, and thickness of the dot are all appropriate, and the anisotropy energy may be neglected.

A number of experiments have been carried out to study nanoscale magnetic systems. Cowburn *et al.* reported magneto-optical measurements on nanoscale supermalloy ($Ni_{80}Fe_{14}Mo_5$) dot arrays (*4*). From the profiles of the hysteresis loops, they concluded that a collinear-type single-domain phase is stabilized in dots with diameters smaller than a critical value (about 100 nm) and that a vortex phase likely occurs in dots with larger diameters. However, the authors were not able to obtain direct information on the spin structure in each dot. As suggested by theoretical calculations, the size of the perpendicular magnetization spot at the vortex core should be fairly small, and hence conventional magnetization measurements should fail to distinguish a fraction of perpendicular magnetization from the surrounding vortex magnetic structure.

In this context, we report magnetic force microscopy (MFM) measurements on circular dots of permalloy ($Ni_{80}Fe_{20}$) that give clear evidence for the existence of a vortex spin structure with perpendicular magnetization core. Samples of ferromagnetic dots were prepared by means of electron-beam lithography and evaporation in an ultrahigh vacuum using an electron-beam gun. The desired patterns were defined on thermally oxidized Si substrates capped by a layer of resist and subsequently topped by a layer of permalloy. By a lift-off process, the resist is removed and permalloy dots with designed sizes remain on top of the Si surface. The thickness of the circular dots reported here is 50 nm; the diameter of the dots was varied from 0.1 to 1 μm. In MFM, the instrument was operated in ac mode to detect the magnetic force acting between the cantilever tip and the surface of the permalloy dots. A low-moment ferromagnetic tip of CoCr was used to minimize the effect of stray fields. The distance between tip and sample surface was set to 80 nm on average. Sample scans

[1]Institute for Chemical Research, Kyoto University, Uji 611-0011, Japan. [2]Faculty of Science and Technology, Keio University, Yokohama 223-8522, Japan.

*To whom correspondence should be addressed. E-mail: shinjo@scl.kyoto-u.ac.jp

†Present address: Research Center Caesar, D-53111 Bonn, Germany.

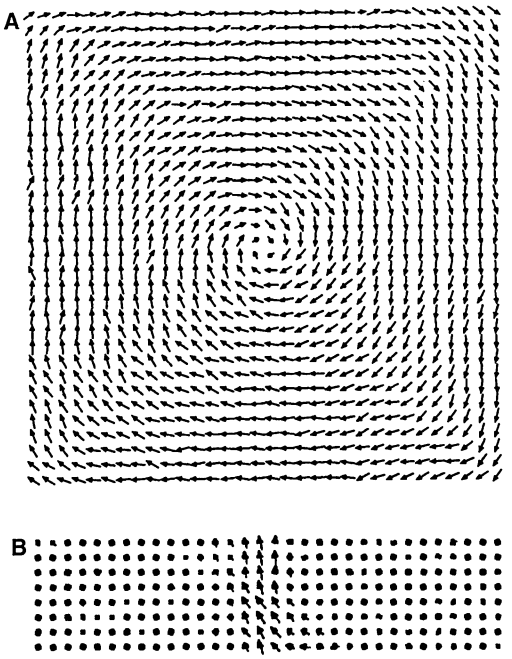

Fig. 1. Monte Carlo simulation for a ferromagnetic Heisenberg spin structure comprising 32 × 32 × 8 spins [courtesy of Ohshima *et al.* (*2*)]. (**A**) Top surface layer. (**B**) Cross-section view through the center. Beside the center, the spins are oriented almost perpendicular to the drawing plane, jutting out of the plane to the right and into the plane to the left, respectively. These figures represent snapshots of the fluctuating spin structure and are therefore not symmetric with respect to the center. The structure should become symmetric by time averaging.

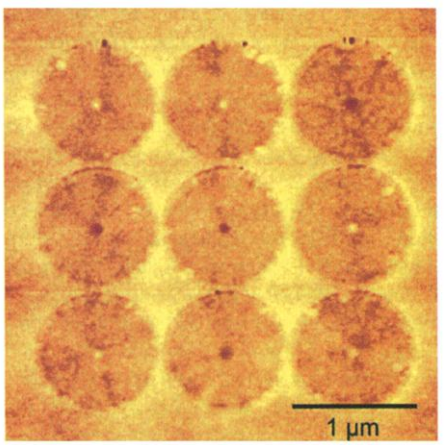

Fig. 2. MFM image of an array of permalloy dots 1 μm in diameter and 50 nm thick.

were taken in air at ambient temperature. An MFM image of an array of 3 × 3 dots of permalloy 1 μm in diameter and 50 nm thick is shown in Fig. 2. For a thin film of permalloy, the magnetic easy axis typically has an in-plane orientation. If a permalloy dot has a single domain structure or shows a domain pattern, in MFM a pair of magnetic poles reflected by a dark and white contrast should be observed in either case. In fact, the image shows a clearly contrasted spot at the center of each dot. It is suggested that each dot has a curling magnetic structure and the spots observed at the center of the dots correspond to the area where the magnetization is aligned parallel to the plane normal. However, the direction of the magnetization at the center seems to turn randomly, either up or down, as reflected by the different contrast of the center spots. This seems to be reasonable, as up- and down-magnetizations are energetically equivalent without an external applied field and do not depend on the vortex orientation (clockwise or counterclockwise). The image shows simultaneously that the dot structures are of high quality and that the anisotropy effective in each dot is negligibly small, which is a necessary condition to realize a curling magnetic structure. (The spots in Fig. 2 around the circumference of each dot are artifacts caused by the surface profile, mainly resulting from unremoved fractions of the resist layer.)

MFM scans were also taken for an ensemble of permalloy dots with varying diameters, nominally from 0.1 to 1 μm (Fig. 3). These images were taken after applying an external field of 1.5 T along an in-plane direction (Fig. 3A) and parallel to the plane normal (Fig. 3B). For dots larger than 0.3 μm in diameter, a contrast spot at the center of each dot can be distinguished, and thus the existence of vortices with a core of perpendicular magnetization is confirmed. Again, the two types of vortex core with up- and down-magnetization are observed (Fig. 3A). In contrast, after applying an external field parallel to the plane normal, all center spots exhibit the same contrast (Fig. 3B), indicating that all the vortex core magnetizations have been oriented into the field direction.

From the above results, there is no doubt that the contrast spots observed at the center of each permalloy dot correspond to the turned-up magnetization of a vortex core. Although the vortex core is almost exactly located at the center of the dot, its real diameter cannot be estimated from the contrast spot observed by MFM, as this is below the lateral resolution power of this technique. To resolve a vortex core by MFM, it is necessary to pin the position of the core so that it is not affected by a stray field from the tip. In the experiments reported above, the vortex cores apparently have been so stable that a clear contrast appears in the MFM imaging process. Magnetic vortices are novel nanoscale magnetic systems, and it will be of great importance in the near future to study the dynamical behavior of turned-up and turned-down magnetizations, that is, fluctuations of the vortex cores.

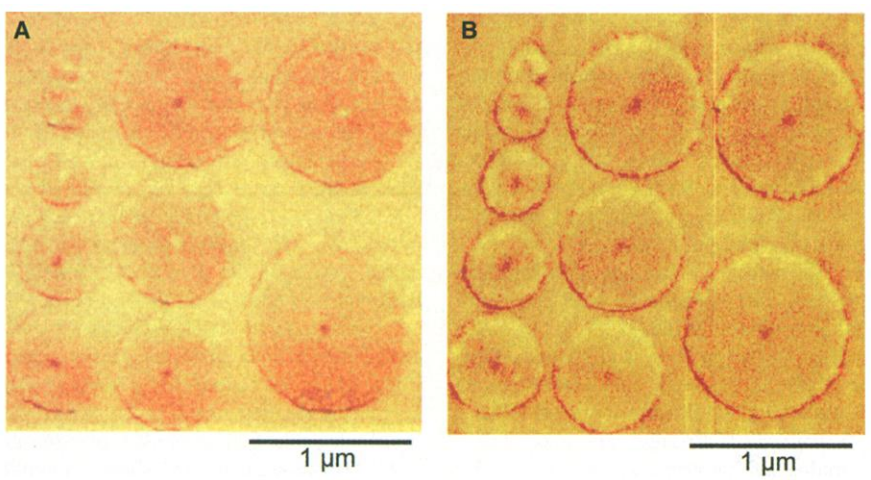

Fig. 3. MFM image of an ensemble of 50-nm-thick permalloy dots with diameters varying from 0.1 to 1 μm after applying an external field of 1.5 T along an in-plane direction (**A**) and parallel to the plane normal (**B**).

References and Notes

1. See, for example, A. Hubert and R. Schäfer, *Magnetic Domains* (Springer, Berlin, 1998).
2. M. Ohshima, N. Suzuki, F. Matsubara, unpublished data.
3. J. Sasaki and F. Matsubara, *J. Phys. Soc. Jpn.* **66**, 2138 (1997).
4. R. P. Cowburn, D. K. Koltsov, A. O. Adeyeye, M. E. Welland, D. M. Tricker, *Phys. Rev. Lett.* **83**, 1042 (1999).

5. We thank F. Matsubara, N. Suzuki, and M. Ohshima for permission to reproduce one of their figures before publication, and Y. Suzuki, P. Beauvillain, J. Miltat, A. Thiaville, N. Hosoito, K. Mibu, S. Isoda, and H. Miyajima for valuable discussions. Supported by a Grant-in-Aid for Creative Basic Research from Monbusho, by the New Energy and Industrial Technology Development Organization (NEDO), and by a Japan Society for the Promotion of Science (JSPS) postdoctoral fellowship (R.H.).

8 March 2000; accepted 14 June 2000

High-Gain Harmonic-Generation Free-Electron Laser

L.-H. Yu,[1]* M. Babzien,[1] I. Ben-Zvi,[1] L. F. DiMauro,[1] A. Doyuran,[1] W. Graves,[1] E. Johnson,[1] S. Krinsky,[1] R. Malone,[1] I. Pogorelsky,[1] J. Skaritka,[1] G. Rakowsky,[1] L. Solomon,[1] X. J. Wang,[1] M. Woodle,[1] V. Yakimenko,[1] S. G. Biedron,[2] J. N. Galayda,[2] E. Gluskin,[2] J. Jagger,[2] V. Sajaev,[2] I. Vasserman[2]

A high-gain harmonic-generation free-electron laser is demonstrated. Our approach uses a laser-seeded free-electron laser to produce amplified, longitudinally coherent, Fourier transform–limited output at a harmonic of the seed laser. A seed carbon dioxide laser at a wavelength of 10.6 micrometers produced saturated, amplified free-electron laser output at the second-harmonic wavelength, 5.3 micrometers. The experiment verifies the theoretical foundation for the technique and prepares the way for the application of this technique in the vacuum ultraviolet region of the spectrum, with the ultimate goal of extending the approach to provide an intense, highly coherent source of hard x-rays.

The invention of the laser provided a revolutionary source of coherent light that created many new fields of scientific research. Modern laser technology provides versatile performance throughout much of the electromagnetic spectrum. Optical resonators exist in the infrared, visible, and ultraviolet regions of the spectrum, whereas nonlinear optics is used to extend coverage toward shorter wavelengths (<200 nm). However, the small nonlinear susceptibilities available at short wavelengths result in inefficient photon up-conversion. Thus, an important objective in optical physics is the development of coherent intense sources at short wavelengths. Work to accomplish this is proceeding in several directions. In particular, there have been advances in high-harmonic (*1*) and x-ray (*2, 3*) sources generated from intense laser-atom interactions and advances in the development of plasma lasers (*4*). However, in the hard x-ray regime (1 Å), the free-electron laser (FEL) emerges as a promising source that is capable of producing unprecedented intensities (*5*). Like synchrotron radiation sources, FELs are based on accelerator technology. FELs represent an advance over synchrotron radiation, because in an FEL the radiation process benefits from multiparticle coherence, whereas synchrotron radiation is emitted incoherently by independently radiating electrons. Consequently, FELs offer the possibility of combining the intensity and coherence of a laser with the broad spectral coverage of a synchrotron.

Several configurations of an FEL source are illustrated in Fig. 1. The most widespread configuration involves the use of a high-Q optical cavity (Q, quality factor) (*6*) and is very effective in wavelength regimes where appropriate mirrors are available. As in the case of lasers, the use of an optical resonator can provide a high degree of spatial and temporal coherence. Conversely, the strategy for developing a hard x-ray FEL (*7*) uses a high-gain, single-pass amplifier scheme to circumvent the lack of high-quality resonator mirrors at short wavelengths. A straightforward approach to single-pass amplification is referred to as self-amplified spontaneous emission (SASE) (*8–21*). In SASE, the spontaneous radiation emitted by quivering electrons near the beginning of a long undulator magnet is subsequently amplified as it copropagates with the electron beam through the magnetic structure. This process is capable of producing output with high peak power and excellent spatial mode, but a limitation imposed by the random noise buildup is poor temporal coherence, i.e., coherence time that is much less than pulse duration.

In this report, we describe an alternative single-pass FEL approach, high-gain harmonic generation (HGHG) (*22–24*), capable of providing the intensity and spatial coherence of SASE but with excellent temporal coherence. Our work was stimulated by earlier theoretical (*25, 26*) and experimental (*27, 28*) studies of harmonic generation. In the HGHG FEL, a small energy modulation is imposed on the electron beam by interaction with a seed laser in a short undulator (the modulator). The energy modulation is converted to a coherent spatial density modulation as the electron beam traverses a dispersion magnet (a three-dipole chicane). A second undulator (the radiator), tuned to a higher harmonic of the seed frequency ω, causes the microbunched electron beam to emit coherent radiation at the harmonic frequency $n\omega$, followed by exponential amplification until saturation is achieved. The HGHG output radiation has a single phase determined by the seed laser, and its spectral bandwidth is Fourier transform limited.

A major advantage of the HGHG FEL is that the output properties at the harmonic wavelength are a map of the characteristics of the high-quality fundamental seed laser. This results in a high degree of stability and control of the central wavelength, bandwidth, energy, and duration of the output pulse. As the duration of the HGHG radiation reflects the seed pulse characteristics, the output radiation pulse can be made shorter than the electron bunch length by simply using an appropriate duration seed laser pulse synchronized to the electron beam. In fact, high-peak-power output pulses of a few femtoseconds are possible with chirped pulse amplification (CPA) (*29*). On the other hand, a short SASE pulse requires an equally short electron bunch, which is presently beyond the state of the art below a few hundred femtoseconds. More problematic is that the temporal profile of the SASE output varies because of the uncontrollable statistical fluctuations of the shot noise that provides the starting signal, and the SASE output is not Fourier transform limited but is a superposition of many wave trains with phases determined by individual electrons.

At the Accelerator Test Facility at Brookhaven National Laboratory, we performed a proof-of-principle experiment to test the theoretical foundations of the HGHG process. By seeding an FEL at a wavelength of 10.6 μm provided by a CO_2 laser, we observed saturated amplified output at the second-harmonic wavelength, 5.3 μm (*30*). The HGHG pulse energy was measured to be $\sim 10^7$ times as large as the spontaneous radiation and $\sim 10^6$ times as large as the SASE signal, which, in the case of the HGHG experiment, provides a background noise.

A schematic of the HGHG apparatus with typical operational parameters is illustrated in Fig. 2 (*31*). The source of the required high-brightness electron beam is the s-band photocathode radio frequency (RF) electron gun (*32*). The 40-MeV electron beam employed in this experiment is characterized by a current of 120 A [0.8 nC in 6 ps full width at half maximum (FWHM)] with a normalized emit-

[1]Brookhaven National Laboratory, Upton, NY 11973, USA. [2]Advanced Photon Source, Argonne National Laboratory, Argonne, IL 60439, USA.

*To whom correspondence should be addressed. E-mail: lhyu@bnl.gov